Magneto-orientational properties of ionically stabilized aqueous dispersions of Ni(OH)2 nanoplatelets

Michael Meyer, Yuryi Raikher, Olivier Sandre, Agnes Bee, Valérie Cabuil, Vincent Dupuis, Pedro Licinio, Régine Perzynski

Eur. Phys. J. E (2008) **26** 335-360
DOI 10.1140/epje/i2007-10338-5

Magneto-orientational properties of ionically stabilized aqueous dispersions of $Ni(OH)_2$ nanoplatelets

M. Meyer[1,2], Yu.L. Raikher[3], O. Sandre[1], A. Bée[1], V. Cabuil[1], V. Dupuis[1], P. Licinio[4], and R. Perzynski[1,a]

[1] Laboratoire des Liquides Ioniques et Interfaces Chargées UMR CNRS 7612, Université Pierre et Marie Curie (Paris 6), ESPCI, case 51, 4, place Jussieu, 75252 Paris Cedex 05, France
[2] LGPMC EA 3325 Université de la Nouvelle Calédonie B.P. R4, 145 ave. James Cook, 98851 Nouméa Cedex, France
[3] Institute of Continuous Media Mechanics, Ural Branch of RAS, 1, Korolyov street, Perm, 614013, Russia
[4] Universidade Federal de Minas Gerais, Instituto de Ciências Exatas, Departamento de Física, av. Antônio Carlos 6628, CP702 Pampulha, 30123-970 Belo Horizonte, MG, Brasil

Received 13 September 2007 and Received in final form 1 February 2008
Published online: 20 June 2008

Abstract. Magnetic and orientational behavior of nickel hydroxide nanoplatelets ionically stabilized in a liquid matrix is studied. Under an applied field the platelets orient their faces normal to its direction. For characterization of the individual behavior of dispersed and non-interacting particles three techniques are used: SAXS, SQUID and magneto-optics. Analysis reveals that nickel hydroxide in a platelet phase is paramagnetic with a pronounced anisotropy of the intrinsic susceptibility, the major component of which (in the direction normal to platelet face) exceeds the minor one by about 25%.

PACS. 82.70.Dd Colloids – 83.80.Hj Suspensions, dispersions, pastes, slurries, colloids – 75.50.Tt Fine-particle systems; nanocrystalline materials – 75.20.Ck Nonmetals

Due to their abilities to self-organize [1,2], concentrated dispersions of nanorods or nanoplatelets raise large scientific and applicational interest. Self-organization of these anisometric (and often intrinsically anisotropic) nano-objects, which are usually sterically stabilized [3–5], results from competition between the orientational entropy favoring the isotropic state, and the excluded-volume entropy favoring a liquid-crystalline order [6]. Aqueous dispersions of clay [7,8] and hexagonal gibbsite [9] are among the very few examples of electrostatically stabilized dispersions of nanoplatelets reported in the literature. In such systems, the effect of shape anisotropy (anisometry) of individual objects on the interparticle interaction is strongly modified by Debye electric screening [10]. Tuning of the latter mechanism allows one to change the interparticle repulsion from strongly anisotropic to roughly isotropic. Accordingly, typical phase diagrams evidence a complicated interplay between nematic and dense gel phases [7–9].

The system described in this paper belongs to this class of ionic colloids. Namely, we study an aqueous dispersion of $Ni(OH)_2$ (nickel hydroxide) nanoplatelets, which in a dilute regime displays very strong field-induced orientational properties. $Ni(OH)_2$ platelets are getting extensively involved as parent systems for manufacturing new types of nanostructured high-discharge capacity battery electrodes [11–13]. An insight to the state of the particles, a deeper understanding of their properties and a possibility to control the internal structure of their dispersions thus seem to be quite timely.

In some aspect, the effects encountered are similar to those reported for lyotropic colloids of mineral particles: goethite nanorods [14], Fe-montmorillonite [15] or gibbsite [16,17]. However, the orientational ordering that takes place in nickel hydroxide nanodispersions is significantly different: under a magnetic field the platelets orient their planes perpendicular to the direction of the latter as if they were striving to build up a diskotic nematic phase.

In what follows, we begin with a brief description of the colloid preparation and the analysis of the morphology and size of the suspended platelets. Then we focus on the magneto-orientational properties of the system which are characterized at room temperature by small-angle X-ray scattering (SAXS) and by magneto-optical birefringence methods. As the particle paramagnetic susceptibility is an issue of our interest, the dilute dispersions of $Ni(OH)_2$ platelets are explored by magnetic SQUID measurements in the temperature range 5–300 K. Finally, the experimental results obtained by different techniques are compared and discussed to identify the individual response (averaged over an ensemble) of $Ni(OH)_2$ platelets to an applied field.

[a] e-mail: regine.perzynski@upmc.fr

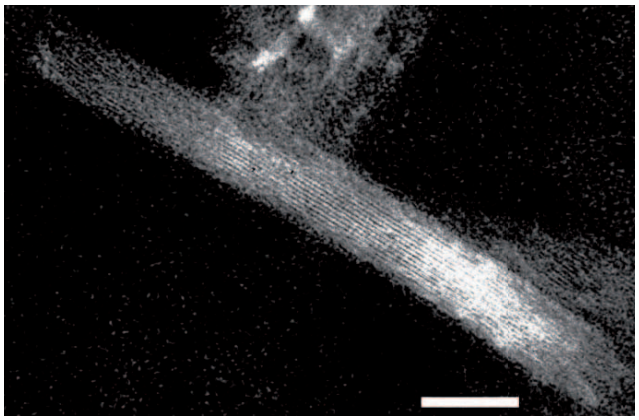

Fig. 1. High-resolution transmission electronic microscopy picture of a side view of a platelet; the measured interplane distance of the crystal lattice is 4.7 Å; the white bar corresponds to 10 nm.

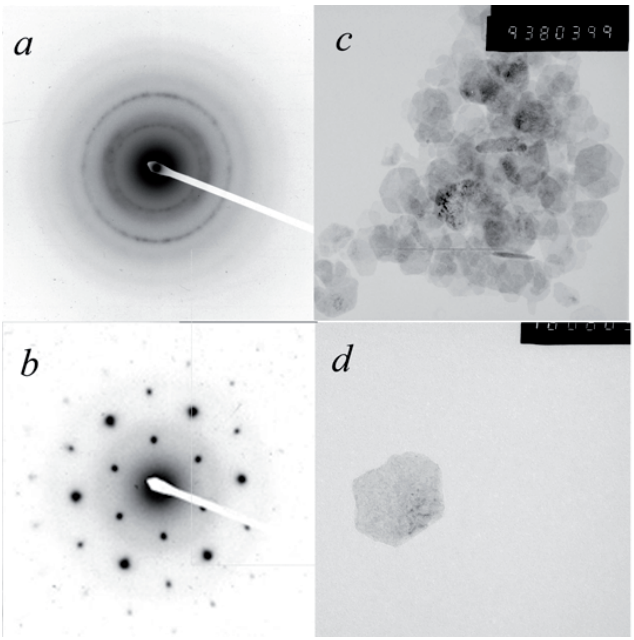

Fig. 2. Transmission electronic microscopy: diffraction (a, b) and pictures (c, d); in (a, c) the beam goes through an ensemble of platelets, in (b, d) the beam is focused on one platelet.

Nickel hydroxide particles are chemically synthesized by adding ammonium hydroxide NH_4OH to a $Ni(NO_3)_2$ solution and heating at 80 °C under vigorous stirring. This synthesis is extensively described elsewhere [18]. Electron microscopy and X-ray diffraction are used to investigate the structure, size and morphology of the obtained objects [18]. Figures 1 and 2 show typical electron transmission micrographs and diffraction patterns of β-$Ni(OH)_2$ platelets, evidencing lamellar structure of spacing ≈ 4.7 Å (close to the bulk value 4.6 Å) and in-plane hexagonal packing. Powder X-ray diffraction (PXRD) of disordered samples, see [18], shows diffraction peaks characteristic of β-$Ni(OH)_2$ structure, enlarged because of the small size of the crystals. The diffraction patterns contain several peaks $[hkl]$ of various widths, which can be indexed. Assuming that the distortion can be neglected, we use Scherrer formalism to deduce the diameter $D = 53 \pm 3$ nm of the platelets from peak [100] (± 3 nm being the uncertainty of the measurement) and their thickness $b = 8 \pm 1$ nm from peak [001]. These determinations are fairly compatible with the typical log-normal diameter distribution $D_0 = \exp(\langle \ln D \rangle) = 55$ nm and width $\sigma = 0.2$ deduced from TEM micrographs, and with Figure 1.

To properly disperse the platelets in water, a sufficiently high surface density of charge is necessary [18,19]. For this purpose, coating with citrate ligands attained by adsorption equilibrium is performed. The volume fraction Φ of the platelets in a stable aqueous dispersion can reach up to 0.15 [19] at $8 < p\mathrm{H} < 12$, while the concentrations of unadsorbed citrate $[\mathrm{cit}]_{\mathrm{free}}$ typically range between $5 \cdot 10^{-3}$ mol/L and $3 \cdot 10^{-2}$ mol/L. The phase diagram as a function of Φ and of the ionic strength of the solution can be found in [19]. In qualitative terms, the dispersions are flowing at low Φ and they are "soft solids" at larger concentrations, the boundary between these two states being ionic strength dependent. As we are interested here in the behavior of individual platelets (averaged in the dispersion over an ensemble of non-interacting particles), we consider very dilute systems with $p\mathrm{H} = 10.5$, where the osmotic pressure is experimentally almost independent of the ionic strength. In this regime the surface charge on the platelets is of the order of $-15\,\mu\mathrm{C/cm^2}$ (meaning roughly one electron charge per $\mathrm{nm^2}$) under the concentration of unadsorbed citrate $[\mathrm{cit}]_{\mathrm{free}} \approx 5 \cdot 10^{-3}$–$3 \cdot 10^{-2}$ mol/L. Quasielastic light scattering experiments, performed on dilute dispersions at $\Phi = 6 \cdot 10^{-4}$ lead to a typical hydrodynamic diameter of 60 nm fully compatible with the powder analysis by TEM and PXRD. It shows that there is no particle aggregation in these dilute dispersions.

Small-angle X-ray scattering measurements under applied magnetic field are performed on D24 beam line in LURE (Laboratoire d'Utilisation du Rayonnement Electromagnétique, Orsay, France). The configuration of the apparatus is tuned to wavelength $\lambda = 0.148$ nm selected by a germanium monochromator with the sample-detector distance 2.76 m. This allows to cover the wave vector interval $6 \cdot 10^{-2}\,\mathrm{nm^{-1}} < q < 1\,\mathrm{nm^{-1}}$. Scattering patterns of the samples at $0.4 \cdot 10^{-2} < \Phi < 2.9 \cdot 10^{-2}$ and $[\mathrm{cit}]_{\mathrm{free}} = 10^{-2}$ mol/L are recorded on a 2D detector with a magnetic field ranging between 0 and 640 kA/m. The signal of the solvent cell is used to subtract the experimental background from the scattering patterns. Being isotropic in zero field, the scattering patterns become anisotropic in its presence. The zero-field measurement allows to determine the form factor of the dispersed objects (data not shown). Because of their polydispersity ($\sigma = 0.2$ from TEM micrographs), this form factor is not oscillatory at large q. We deduce the gyration radius $R_g = 20 \pm 1$ nm of the nanoplatelets from the slope $-R_g^2/3$ of a semi-logarithmic plot of the intensity as a function of q^2 in the range $qR_g \leq 2$. Their thickness $b = 6.1 \pm 0.3$ nm is measured in the intermediate q regime $\pi/R_g < q < \pi/b$ from the slope $-b^2/12$ of a Kratky-Porod plot $\ln(Iq^2)$ *vs.* q^2, which

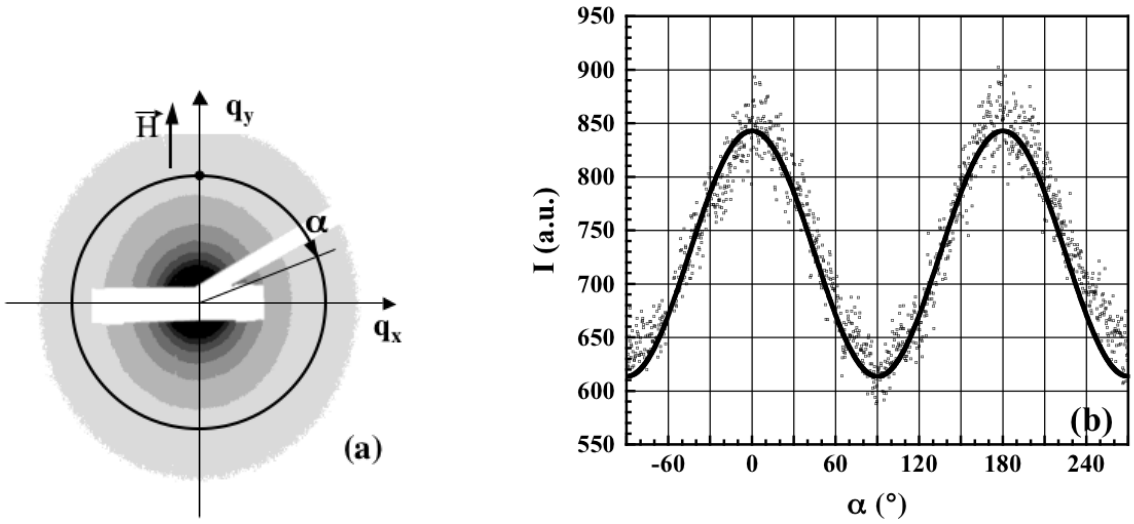

Fig. 3. SAXS scattering for a $Ni(OH)_2$ platelet suspension at $\Phi = 2.9 \cdot 10^{-2}$ and $[\text{cit}]_{\text{free}} = 10^{-2}$ mol/L in a field $H = 640$ kA/m; (a) the scattering pattern elongated along the field direction (to better reveal the anisotropy, a greyscale with only 8 levels is used); α is the azimuth angle defined in the text; (b) the angular dependence of the scattered intensity I at a given scattering vector $q = 0.29\,\text{nm}^{-1}$ fitted with the aid of formula (1). Its experimental value at $H = 0$ is 680 a.u.

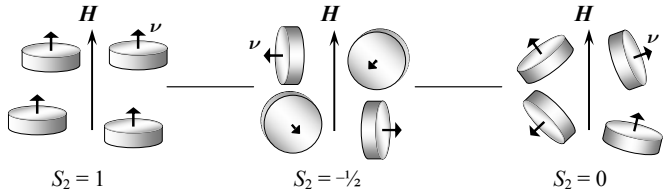

Fig. 4. Schematic view of orientational distributions of the platelets in a liquid matrix corresponding to the limiting values of the orientational order parameter (left to right): easy-axis, easy-plane, disordered.

confirms the platelet shape of the dispersed objects. We then calculate the nanoplatelet diameter $D = 56 \pm 3$ nm using the expression $R_g^2 = D^2/8 + b^2/12$ assuming axial symmetry of the dispersed objects. This value of D agrees fairly well with other our measurements. Figure 3a illustrates the anisotropy of the scattering pattern for a sample of $\Phi = 2.9 \cdot 10^{-2}$ under a field $H = 640$ kA/m. The pattern is elongated along the direction of the applied field $\boldsymbol{h} = \boldsymbol{H}/H$, meaning that the platelets orient their major dimension perpendicular to the field. The scattering intensity at a given q value varies along the azimuthal angle according to [17,20]

$$I(q, H, \alpha) = I(q, H = 0)\left[1 - (1 - 3\cos^2\alpha)\, S_2(H)\right], \quad (1)$$

where $I(q, H = 0)$ denotes the isotropic value of I in the absence of field and $S_2 = \frac{3}{2}[\langle(\boldsymbol{\nu h})^2\rangle - \frac{1}{3}]$ is the orientation order parameter built on unit vector $\boldsymbol{\nu}$ normal to the platelet face and defined as a statistical average over the particle ensemble; the azimuthal angle is $\alpha = \arccos[(\boldsymbol{qh})/q]$. The orientational structures corresponding to the limiting values of the order parameter S_2 are shown in Figure 4.

Figure 3b shows a fit with equation (1) of the data of Figure 3a recorded on the 2D detector along a full circle at $q = 2.9\,\text{nm}^{-1}$ under $H = 640$ kA/m. The value of the orientation order parameter rendered by this adjustment is $S_2 = 0.096$. At constant H, the parameter S_2 with the accuracy $\pm 8\%$ depends neither on q nor on Φ within the respective ranges investigated. Figure 5a presents the field dependence of S_2; the data scale as H^2, confirming that we deal with a polarizable system. As seen from Figure 5a, the observed value of S_2 is always positive, in contrast to what was obtained with goethite nanorods in [10], where a non-monotonic behavior was observed. Moreover, as $S_2(H)$ is found to be independent of both q and Φ, one concludes that the orienting entities indeed possess shape anisotropy and behave independently.

The individual field-induced behavior is confirmed by another experiment, which is also sensitive to the parameter S_2, but which is based on a completely different technique and range of wavelengths. Namely, with a set-up detailed in [21], a magneto-optical measurement is performed. We find that under an applied magnetic field varying between 0 and 900 kA/m, dilute dispersions of $Ni(OH)_2$ platelets display an optical birefringence Δn which is negative. In the experimental range of H and Φ, the induced optical anisotropy Δn is proportional to the square of the applied field, see Figure 5b, and linear in the volume fraction Φ of the dispersed particles. Birefringence of such a type implies that under field a progressive orienting of the objects with a negative intrinsic optical anisotropy takes place. Given that, the attained optical anisotropy takes the form

$$\Delta n = -|\delta n_o| \Phi\, S_2(H), \quad (2)$$

where the intrinsic anisotropy δn_o is a function of the particle shape and of its intrinsic refraction index. Substituting in equation (2) the obtained SAXS results, one obtains for the mean value of the intrinsic anisotropy the estimate $\delta n_o = -0.05 \pm 0.005$. We note that the

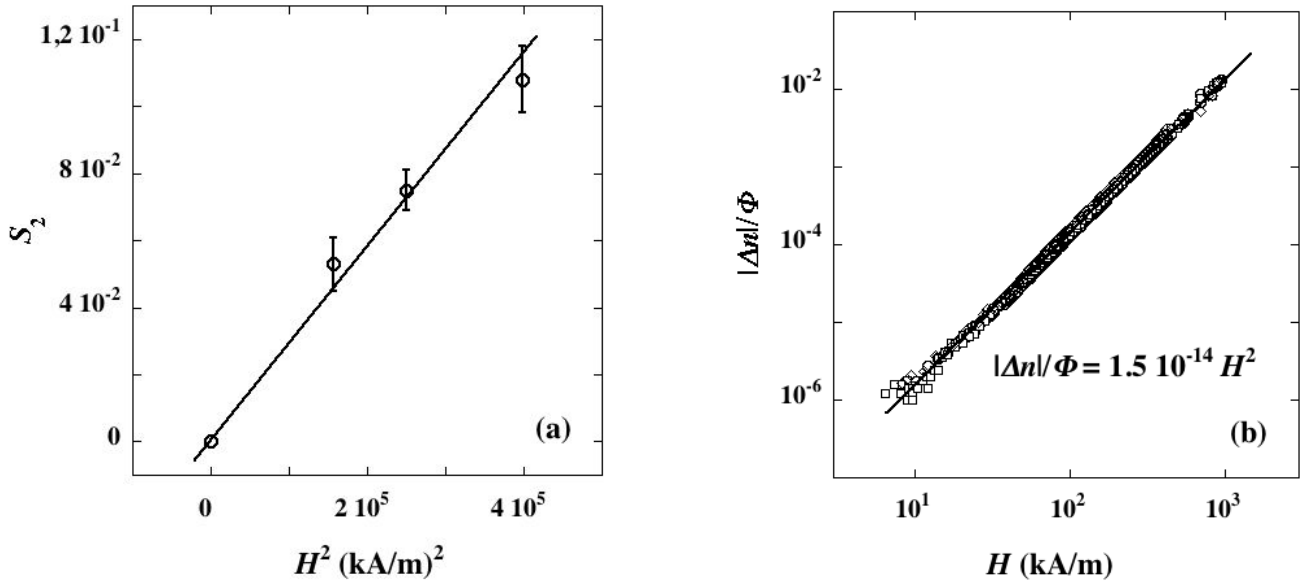

Fig. 5. Field dependences: (a) of the orientation order parameter S_2. For each value of the field, S_2 is averaged over $0.15\,\mathrm{nm}^{-1} < q < 0.3\,\mathrm{nm}^{-1}$ and $0.4 \cdot 10^{-2} < \Phi < 2.9 \cdot 10^{-2}$; measurements are done at $[\mathrm{cit}]_{\mathrm{free}} = 10^{-2}\,\mathrm{mol/L}$. The full line corresponds to $S_2 = 2.9 \cdot 10^{-7}\,H^2$, where H is taken in kA/m; (b) of the reduced magnetic birefringence $\Delta n/\Phi$ for three different samples at $\Phi = 0.5\% \pm 0.1\%$ with $5 \cdot 10^{-3}\,\mathrm{mol/L} < [\mathrm{cit}]_{\mathrm{free}} < 10^{-2}\,\mathrm{mol/L}$.

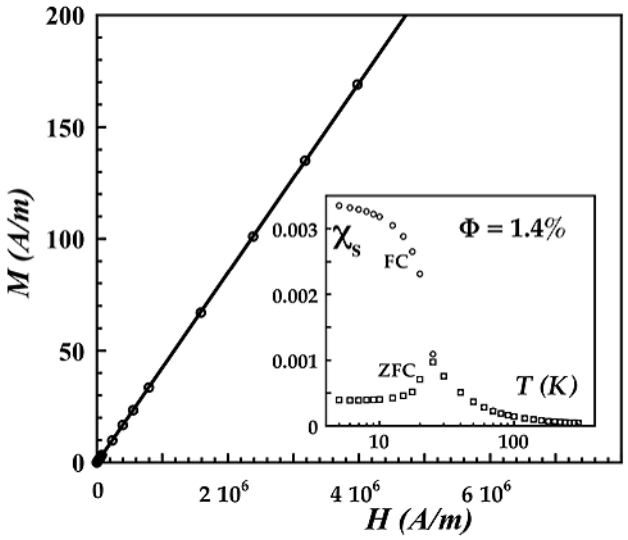

Fig. 6. Magnetization of a dispersion of platelets at $\Phi = 1.4\%$ and $[\mathrm{cit}]_{\mathrm{free}} = 2.6 \cdot 10^{-2}\,\mathrm{mol/L}$ at room temperature. Inset: temperature dependence of the initial susceptibility of the same sample measured at $H = 4.1\,\mathrm{kA/m}$ under field-cooled (circles) and zero-field-cooled (squares) regimes.

field-induced orientation reported here is essentially different from the one obtained in [15,16], where the platelets positioned their flat faces parallel to the field. The explanation is that the mineral microdisks in [16] are diamagnetic; hence, due to the shape effect, their field-induced dipoles align with the major dimension of the object.

In principle, the experimentally established facts of $S_2(H)$ being positive and δn_{o} negative, could be accounted for with the aid of two alternative models. One assumes that the particles have permanent magnetic moments directed along $\boldsymbol{\nu}$. The second one is based on the platelets being paramagnetic with the intrinsic susceptibility tensor possessing a pronounced anisotropy. However we have not found any indications of permanent magnetic moments neither in our measurements at room temperature (see just below) nor in the literature. According to [22–25], where magnetic properties of disperse $\mathrm{Ni(OH)_2}$ were investigated quite thoroughly at 4–300 K, the particles lose global antiferromagnetism at about 20 K and any signs of metamagnetic behavior at about 100 K. This eliminates any hypothesis of existence of a spontaneous magnetic moment, and makes the anisotropic paramagnetic model with the maximum component $\chi_{\parallel}$ of intrinsic susceptibility along the normal $\boldsymbol{\nu}$ to the platelet the only plausible one.

Magnetization measurements performed with a SQUID (Superconducting Quantum Interference Device, Quantum Design, MPMS) confirm the paramagnetic nature of the response of dilute dispersions of $\mathrm{Ni(OH)_2}$ to an applied field at room temperature. As follows from Figure 6, the magnetization of a colloid with volume fraction $\Phi = 1.4\%$ is proportional to the applied field up to $H = 4 \cdot 10^3\,\mathrm{kA/m}$. Using the data presented in this figure, we obtain for the susceptibility of the suspension in the direction of the field $\chi_s = M/H = 4.2 \cdot 10^{-5}$. The equilibrium susceptibility of a suspension of uniaxially anisotropic paramagnetic particles subjected to Brownian rotary motion depends on the orientation order parameter in the following way [26]:

$$\chi_s = \Phi \left[\chi_\perp + \left(\tfrac{2}{3} S_2 + \tfrac{1}{3} \right) \Delta\chi \right], \qquad (3)$$

where $\chi_\perp$ is the susceptibility per unit volume of the platelet in the direction perpendicular to $\boldsymbol{\nu}$, and $\Delta\chi =$

$\chi_\parallel - \chi_\perp$. Since the orientation order parameter S_2 grows with H, the susceptibility (3) is weakly field dependent.

Assuming proportionality of the field-induced magnetization to the particle volume fraction, one obtains the paramagnetic susceptibility of the particle substance

$$\chi = \chi_s/\Phi = (3.0 \pm 0.1) \cdot 10^{-3}; \tag{4}$$

here a possible correction due to shape anisotropy is negligible. The estimate given by equation (4) agrees fairly well with the value $\chi = 2.6 \cdot 10^{-3}$ found in magnetic measurements of [24] on dense $Ni(OH)_2$ gels at 300 K under much weaker field $H = 280\,\mathrm{kA/m}$. For a particle with an anisotropic paramagnetic susceptibility embedded in a liquid matrix, the orientation-dependent part of Zeeman energy is

$$U = -\tfrac{1}{2}\mu_0 \Delta\chi V H^2 (\boldsymbol{\nu h})^2, \tag{5}$$

where V is the particle volume. Performing statistical averaging over the particle orientation angle with the Boltzmann distribution $W \propto \exp(-U/kT)$ and expanding the result for $\Delta\chi V H^2/kT < 1$, one finds for the orientation order parameter

$$S_2(H) = \frac{\mu_0 \Delta\chi V H^2}{15kT}\,. \tag{6}$$

Modeling our objects as identical round cylinders and using the particle size measurements, one finds $V \sim 2 \times 10^{-23}\,\mathrm{m}^3$. Further, from $S_2(640\,\mathrm{kA/m}) = 0.1$ with the aid of equation (6) one arrives at the estimate $\Delta\chi \approx 6 \times 10^{-4}$. This means that the intrinsic magnetic susceptibility tensor for the platelet phase of $Ni(OH)_2$ is of the form

$$\chi_{ik} = \chi_\perp \delta_{ik} + (\chi_\parallel - \chi_\perp)\,\nu_i \nu_k, \tag{7}$$

with $\chi_\perp \approx 2.7 \cdot 10^{-3}$ and $\chi_\parallel/\chi_\perp \approx 1.25$. Under thermalization in the absence of the field the net value of the initial susceptibility of a colloid should be $\chi_s = \frac{1}{3}\Phi(\chi_\parallel + 2\chi_\perp)$, that is about $2.9 \cdot 10^{-3}\Phi$. Experimentally, with the given accuracy this value is hardly distinguishable from the one of equation (4). This is understandable as the degree of orientation in the suspension of paramagnetic particles is not high: $\sim 10\%$. However SAXS and birefringence experiments, being sensitive exclusively to S_2, unambiguously prove its existence.

Crystallographic data confirms that in the platelets the axis $\boldsymbol{\nu}$, *i.e.*, the normal to the particle face, is singled out. Indeed, it is well known, see [24,25] for example, that the platelet crystal is a layered structure with a hexagonal in-layer packing of Ni atoms. In the antiferromagnetic state at low temperatures, the c-axis becomes the easy axis of magnetic anisotropy. Although at room temperature there is no spontaneous spin ordering, it is reasonable to suppose that the spin-orbit interaction is still present, and the field-induced paramagnetic polarization is enhanced in the direction of the crystal field.

The temperature dependence of the field-cooled (FC) and zero-field-cooled (ZFC) susceptibilities in the temperature range 5–300 K in the field $H = 4.1\,\mathrm{kA/m}$ are also investigated. The results are presented in the inset of Figure 6. The magnetic behavior at high temperatures is typically paramagnetic: FC and ZFC magnetizations coincide and behave as $1/T$. At low temperatures, the FC magnetization continuously increases as the temperature is decreased which most probably indicates metamagnetic behavior. On the other hand, the ZFC magnetization presents a peak at a temperature 25 K, which matches closely the Néel point T_N for the low-temperature antiferromagnetic phase which does not differ greatly for the platelet and bulk phases, see [22–25]. However, already in [24] some indications of appearance of particle spontaneous magnetic moments below T_N were mentioned. This was at the time when Néel was preparing his concept [27] according to which fine grains of an antiferromagnet always acquire permanent magnetic moments of the order $\mu_A N^p$, where μ_A is the magnetic moment of a sublattice atom, N the total number of such atoms in the grain, and $\frac{1}{3} < p < \frac{2}{3}$. By now this fact is well established for ferric hydroxides like ferrihydrite and mineral cores of ferritin [28]. It seems that in nickel hydroxide the electron magnetic resonance could be an appropriate tool to provide the evidence for the existence of such states and to monitor their behavior as a function of temperature, as it is for ferrihydrite [29].

Conclusions

Individual magnetic and orientational behavior of nickel hydroxide nanoplatelets is studied by means of stabilizing particles in a liquid matrix. For characterization of the particles three independent techniques are used: SAXS, SQUID and colloid magneto-optics. Under an applied field the suspended platelets orient their faces normal to the field direction; the order parameter attained under $H = 640\,\mathrm{kA/m}$ at room temperature is about 0.1. Analysis of this effect is performed by combining the results of all the aforementioned measurements. It reveals that nickel hydroxide in a platelet phase is paramagnetic with a pronounced anisotropy of the intrinsic susceptibility. The field-induced orientation in a dilute dispersion of $Ni(OH)_2$ has the same symmetry as the liquid-crystalline ordering arising spontaneously in dense assemblies of same particles. This infers that a magnetic field is an important controlling factor which can either reduce the critical concentration (at given temperature) or increase the reference temperature (at given concentration) of the liquid-crystalline transition in $Ni(OH)_2$ platelet systems. Low-temperature magnetic measurements indicate that below 100 K the particles develop metamagnetic and antiferromagnetic properties. Further studies of these phenomena seem to be very promising.

Partial support of the work by ECO-NET Program No. 16274QL is gratefully acknowledged. Y.R. acknowledges also support on the part of UrB/SB RAS Collaboration Program and RFBR project 07-02-96026. P.L. acknowledges support from CAPES 1973/01-0, all the authors thank C. Bourgaux for providing help on D24 beam line in LURE and N. Malikova for careful re-reading of the manuscript.

References

1. I. Langmuir, J. Chem. Phys. **6**, 873 (1938).
2. J.C.P. Gabriel, P. Davidson, Adv. Mater. **12**, 9 (2000).
3. F.M. van der Kooij, K. Kassapidou, H.N.W. Lekkerkerker, Nature **406**, 868 (2000).
4. A.B.D. Brown, C. Ferrero, T. Narayanan, A.R. Rennie, Eur. Phys. J. B **11**, 481 (1999).
5. A.B.D. Brown, S.M. Clarke, A.R. Rennie, Langmuir **14**, 3129 (1998).
6. L. Onsager, Ann. N.Y. Acad. Sci. **51**, 627 (1949).
7. L.J. Michot, I. Bihannic, K. Porsch, S. Maddi, C. Baravian, J. Mougel, P. Levitz, Langmuir **20**, 10829 (2004).
8. C. Martin, F. Pignon, J.-M. Piau, A. Magnin, P. Lindner, B. Cabane, Phys. Rev. E **66**, 021401 (2002).
9. D. van der Beek, H.N.W. Lekkerkerker, Europhys. Lett. **61**, 702 (2003).
10. E. Trizac, L. Bocquet, R. Agra, J.J. Weis, M. Aubouy, J. Phys.: Condens. Matter **14**, 9339 (2002).
11. X.Liu, L. Yu, Mater. Lett. **58**, 1327 (2004).
12. X. Liu, G. Qiu, Z, Wang, X. Li, Nanotechnology **16**, 1400 (2005).
13. G. Xiao-yan, D. Jian-cheng, Mater. Lett. **61**, 621 (2007).
14. B.J. Lemaire, P. Davidson, J. Ferré, J.P. Jamet, P. Panine, L. Dozov, J.P. Jolivet, Phys. Rev. Lett. **88**, 125507 (2002).
15. F. Pignon, A. Alemdar, A. Magnin, T. Narayanan, Langmuir **19**, 8638 (2003).
16. D. van der Beek, Thesis, Utretch University, Netherlands (2005).
17. D. van der Beek, A.V. Petukhov, P. Davidson, J. Ferré, J.P. Jamet, H.H. Wensink, G.J. Vroege, W. Bras, H.N.W. Lekkerkerker, Phys. Rev. E **73**, 041402 (2006).
18. M. Meyer, A. Bée, D. Talbot, V. Cabuil, J.M. Boyer, B. Répetti, R. Garrigos, J. Colloid Interface Sci. **277**, 309 (2004).
19. M. Meyer, Thèse, Université Paris 6, France (2003).
20. K.R. Purdy, Z. Dogic, S. Fraden, A. Rühm, L. Lurio, S.G.J. Mochrie, Phys. Rev. E **67**, 031708 (2003).
21. E. Hasmonay, E. Dubois, J.C. Bacri, R. Perzynski, Yu.L. Raikher, V.I. Stepanov, Eur. Phys. J. B **5**, 859 (1998).
22. T. Takada, Y. Bando, M. Kiyama, H. Miyamoto, T. Sato, J. Phys. Soc. Jpn. **21**, 2745 (1966); H. Miyamoto, Mat. Res. Bull. **11**, 599 (1976).
23. T. Enoki, I. Tsujikawa, J. Phys. Soc. Jpn. **45**, 1515 (1978).
24. J.T. Richardson, W.O. Milligan, Phys. Rev. **102**, 1289 (1956).
25. A. Szytula, A. Murasik, M. Balanda, Phys. Status Solidi (b) **43**, 125 (1971).
26. Yu.L. Raikher, V.I. Stepanov, Adv. Chem. Phys. **124**, 419 (2004).
27. L. Néel, C. R. Acad. Sci. (Paris) **252**, 4075 (1961).
28. M.S. Seehra, A. Punnoose, Phys. Rev. B **64**, 132410 (2001).
29. A. Punnoose, M.S. Seehra, J. van Tolc, L.C. Brunel, J. Magn. & Magn. Mater. **288**, 168 (2005).